IEEE Access
Multidisciplinary | Rapid Review | Open Access Journal

Received 30 June 2022, accepted 21 July 2022, date of publication 1 August 2022, date of current version 4 August 2022.

Digital Object Identifier 10.1109/ACCESS.2022.3195296

RESEARCH ARTICLE

Experimental Verification of the Modified PSA Algorithm

XIAO LI[1], LIQIANG WANG[1], AND MUNYARADZI MUNOCHIVEYI[2]
[1]School of Electronic Engineering, Tianjin University of Technology and Education, Tianjin 300222, China
[2]Department of Electrical and Electronic Engineering, University of Zimbabwe, Harare, Zimbabwe

Corresponding author: Liqiang Wang (wangliqiang@tute.edu.cn)

ABSTRACT Being abundant and non-polluted, solar energy is an increasingly desirable energy source. Growing research is concerned about maximum solar energy acquisition from solar panels, especially in the automatic sun-tracking of the solar panels. This paper presents a modified algorithm based on the ''PSA algorithm'' proposed in the 2001, and presents a new automatic solar tracking system with a two-axis is designed based on the algorithm. The PSA modified algorithm is used to calculate the sun's horizontal azimuth and zenith angle combined with time, longitude, latitude, and other information. This experiment of the prototype mainly composed of a microcontroller, a global positioning system (GPS) module, a digital compass, a tilt sensor, a 555 timer, and gates, optical couples, a H-bridge and two stepper motors. Then a series of experiments are conducted using the proposed prototype in Tianjin City. Measured zenith angle values were collected and recorded based on the PSA modified algorithm and the original PSA algorithm, compared with the actual Zenith Angle of the Sun in Tianjin City. The comparison curves of Zenith Angle show that the measurement accuracy of the modified PSA algorithm is higher than that of the PSA original algorithm.

INDEX TERMS Automatic solar tracking system, measurement accuracy, PSA modified algorithm, two-axis tracking method, zenith angle.

I. INTRODUCTION

Solar energy is cost-effective, reliable, nonpolluting, and widely accepted when compared to other forms of renewable energy. Solar systems have been developed for different applications in industrial and domestic settings. The solar systems act as a collector, which captures solar energy and converts it into thermal or electrical energy [1]. The produced power depended on the total energy captured by the collector. The integration of a tracking system to a solar energy system helps to increase the output [2]–[10]. The system helps to orient a photovoltaic (PV) panel or collector, in the radiation beam direction of the Sun. The Sun with respect to the Earth changes both with time and season, as the Sun moves around the Earth. Related works about solar trackers can be defined as either active/passive or single/two-axis based [11]–[14]. Trackers with single-axis tracking usually have manual elevation capability on a second axis which can be tuned regularly throughout the year. Also, single-axis trackers have two types of tracking, polar and horizontal. Whilst the two-axis tracker moves horizontally or vertically.

Sun trackers orient the solar system to make up for the motion, thereby maintaining the system directly pointed at the beam of radiation from the Sun. Generally, a useful tracking system can reorient itself to benefit from diffuse solar radiation emitted under cloudy conditions. The tracking systems can be classified as either passive/active tracking systems utilizing an open/closed-loop approach [15]. Some works have also discussed hybrid systems based on both active and passive tracking methods [16]. Solar trackers can boost energy gain, however, there are cost, reliability, energy consumption, and maintenance problems that must be considered. Therefore, tracking systems should be designed to ensure the tracking method increases the power gain instead of decreasing it. In the modern field of solar tracking technology, many domestic and foreign scholars have carried

The associate editor coordinating the review of this manuscript and approving it for publication was Geng-Ming Jiang.

out long-term and effective research on the design of the mechanical structure, ray-tracking method and controlling system. There are mainly receiving devices of fixed, uniaxial, and biaxial tracking types. The uniaxial tracking system can receive more solar energy than the fixed tracking system [17]–[19], the studies presented in [17] improved the accuracy of a uniaxial tracking type by 0.5°. Also, experimental results from a variety of different mechanical structures indicate that the biaxial tracking system can receive more energy than the fixed solar system by 30% to 40% [5]. Photoelectric and trajectory tracking are two dominant ray tracking methods and obtain remarkable advantages, compared to the common tracking methods that rely on the longitude and latitude of the tracking region [20]. When the location of the tracker is changed, the controlling program must be changed too, which is inconvenient for tracking. This means that the Global Positioning System (GPS) module becomes crucial because it can provide real-time longitude and latitude information of the tracking area no matter where the tracking device is located. A major obstacle to the adoption of a sensor-based solar tracking system is mainly its high cost, due to the high cost of light sensors following the Sun's apparent position in cloudy conditions. Hence, the positioning algorithm applied in the solar tracking system has a direct influence on the measurement accuracy of the Sun's position. In literature, a new calculation-based approach has been proposed, they demonstrated that the proposed tracker can track the Sun satisfactorily without using sensors, therefore, making automatic sun trackers affordable for developing communities [21]. A low-cost biaxial tracking scheme based on the Astronomical Almanac's algorithm is proposed in recent years, the system outperformed fixed systems by 13.9% and optical-sensor systems by 2.1% [22]. Another recent study in [23]–[25], proposed a tracking algorithm focused on computing the Sun's position via rectangular coordinates.

Also, the spencer formula is most cited solar declination method. The Spencer's formula achieves 3 minutes of arc maximum declination error and 35 seconds of timing error and as the days vary continuously over time, the error in Spencer's formula can become as great as 0.28 degrees. Motivated by this, they developed the position solar algorithm (PSA) [26]. In [26] authors investigated several relevant sun position algorithms and proposed a new algorithm, denoted as the ''PSA Algorithm''. This algorithm was designed to be efficient computationally and highly accurate. Consequently, because of the algorithms' good balance between computational speed and accuracy, the PSA algorithm can still be found in many solar tracking devices and systems. However, the PSA algorithm was designed to predict the true solar vector within 0.5 minutes of arc in the period from 1999 to 2015 [27]. Moreover, the authors note that the PSA algorithm in the period 2020–2050 succumbs to a maximum angular deviation error of 35 arcsec with respect to the true solar vector. PSA algorithm can predict solar vectors with high accuracy between 1999 - 2015. Therefore, it would be fairer and more accurate to compare the presented variant the modified PSA predicts the solar vector with high accuracy in the 2020-2050 range. In [28] authors proposed five solar energy position calculation methods and to comparison with existing algorithms and that three most methods (Michalsky, PSA, ENEA) declare maximum errors of 0.01°, 0.008° and 0.0027°, respectively, their validity time ranges are 1950–2050, 1995–2015, 2003–2023. In [29] authors described a procedure for a Solar Position Algorithm (SPA) to calculate the solar zenith and azimuth angle with uncertainties equal to ±0.0003 and summarized the complex algorithm elements scattered throughout the book to calculate the solar position. However, the algorithm in the report is more complex than that in this paper. In [26] authors reviewed various algorithms currently available in the solar literature and a new algorithm, developed at the Plataforma Solar de' ukAlmeria, which combines these two characteristics of accuracy and simplicity, is presented. The algorithm allows of the true solar vector to be determined with an accuracy of 0.5 minutes of arc for the period 1999–2015. Poulek in 1994, designed and tested a single axis passive solar tracker using shape memory alloy actuators. The alloy can be easily deformed even under 70 degrees Celsius. It returns to its original shape when heated above its transformation temperature. The efficiency was reported to be almost 2% and two orders of magnitude better than bimetallic actuators [30]. Also, Clifford *et al.* then designed a new low-cost solar tracker suitable for use in equatorial regions. The solar tracker is passively activated by aluminum/steel bimetallic strips and controlled by a viscous damper to prevent oscillation. Computer modeling is used to compare with the experimental results. Through computer simulation, the efficiency is improved by 23% compared with the fixed solar panel, which is consistent with the experimental results [31].

Motivated by the above discussion, in this paper, we present a modified version of the PSA algorithm that based on this original algorithm, we designed and prototyped an automatic solar tracking system, our proposed system is shown in Fig. 1 to test the effectiveness of our proposed modified PSA algorithm. The solar tracking system's maximum power is 48W, and the minimum power is 20W. The proposed automatic solar system, includes a microcontroller, a GPS module, a digital compass, a tilt sensor, a 555 timer, and gates, optical couples, an H-bridge and two stepper motors and power. The microcontroller receives information from the GPS module to obtain the real-time solar position and the digital compass measures the horizontal azimuth of the solar panel and the tilt sensor measures its zenith. Thus, by comparing the data measured with the position calculated, one can determine the accuracy of the proposed algorithm for sun-tracking. Consequently, our results demonstrate that our proposed algorithm maintains the same computational efficiency while performing significantly better in the period 2021–2050. Even though, in recent years, sun-tracking PV panels are rarely seen in practice as the cost of PV panels has dramatically decreased in the past five years. However, accurate sun-tracking is still important for high solar

concentrating systems, therefore, the algorithm that we proposed can provide potential benefit for such systems due to the improvement in sun-tracking provided by our solution.

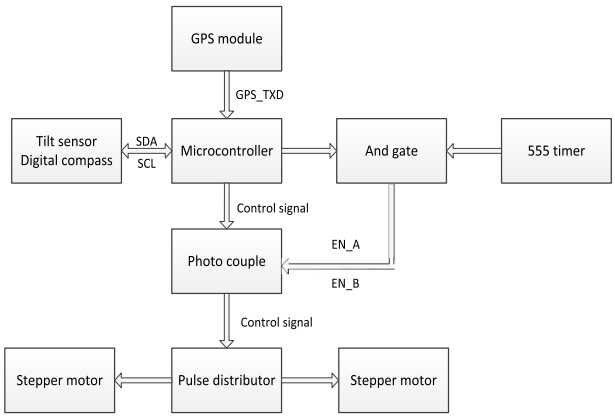

FIGURE 1. Block diagram of the automatic solar tracking system.

II. TRACKING ALGORITHM FOR CALCULATING THE SOLAR POSITION

This section begins with a brief explanation of some of the terms used in the algorithm and then the PSA original algorithm and the PSA modified algorithm will be introduced in detail.

A. SEVERAL KEY TERMS USED IN THE ALGORITHM

1) EARTH-SUN GEOMETRY

The orbit around the Sun is denoted as the Ecliptic is shown in Fig. 2. The celestial equator is the representation of the Earth's equatorial plane as it is projected to infinity. The equinoxes represent the intersection of this plane with the ecliptic. Fig. 2 also shows the earth at the vernal and autumnal equinoxes and the obliquity of the ecliptic is the angle between the ecliptic and equatorial plane. In addition, in the southern hemisphere, the vernal equinox marks the beginning of summer, and the autumnal equinox corresponds to the beginning of winter. 23 September and 21 March are days vernal and autumnal equinoxes, respectively, occur approximately.

2) LATITUDE AND LONGITUDE

Three basic coordinate systems which are used in the solar position determination, are longitude/latitude for positions on the earth, right ascension/declination for celestial objects positions and azimuth and zenith angle for the Sun. In this work, we measure longitude from the Greenwich meridian, and latitude from the equator. Thus, longitude and latitude can be used to determine any position on the Earth's surface.

3) RIGHT ASCENSION AND DECLINATION COORDINATES

The right ascension/declination coordinate system is like the longitude/latitude system discussed above. In more detail, the right ascension is the angle from the vernal equinox eastward towards the celestial equator to the junction with the declination circle, and declination as the angle from the celestial equator to the object (positive north), subtended at the center of the celestial sphere. RA as the right ascension and DECL as the declination is shown in Fig. 3.

The right ascension varies depending on the earth's orbital position. For stars, due to the large distances between the earth and stars, the earth-sun distance introduces negligible errors for the right ascension/declination for all but the most precise applications. However, this is not the case for the Sun, as the distance is small compared to the stars. Thus, the Sun's right ascension/declination varies daily.

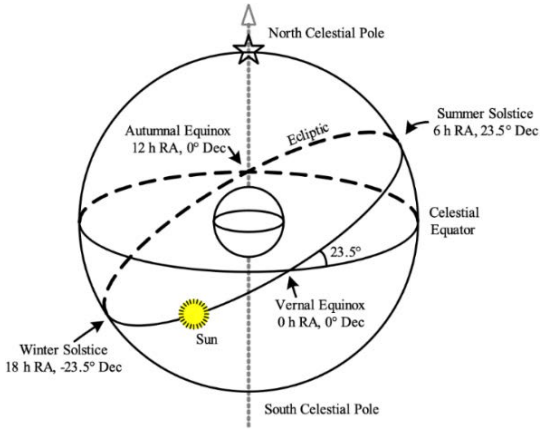

FIGURE 2. Position of equinoxes.

4) AZIMUTH AND ZENITH ANGLE

The zenith is defined as the Sun's incidence angle and the azimuth angle as the horizontal plane traversing clockwise from the north to the Sun's center. The elevation angle is determined as shown in Fig. 4 and Fig. 5, is the zenith angle, is the azimuth angle and is the elevation angle.

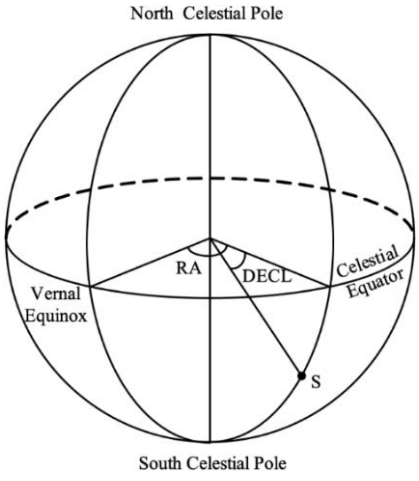

FIGURE 3. Right ascension and declination.

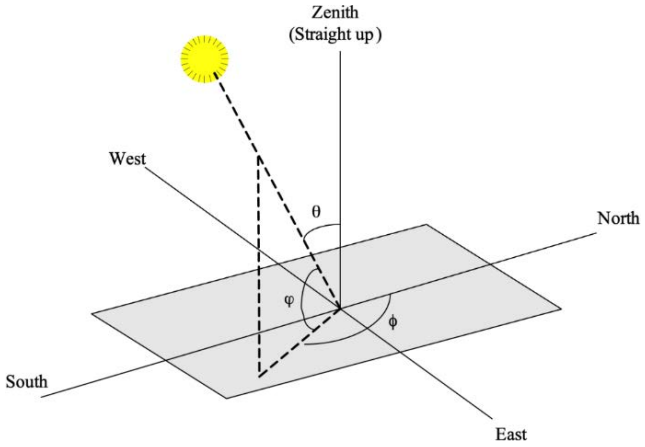

FIGURE 4. Diagram showing Zenith and Azimuth angle.

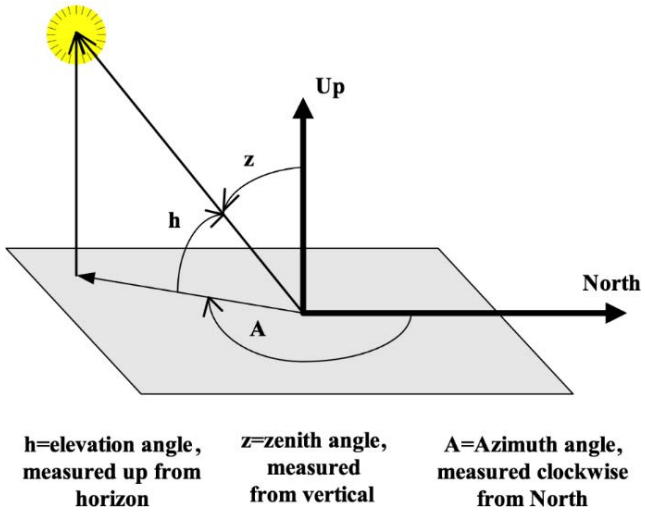

FIGURE 5. Angles of Sun position.

B. PSA MODIFIED ALGORITHM

The position of the Sun in the sky depends on the following:

1) Time.
2) The motion of planets around the Sun.
3) Seasons.
4) Observer location.

The first input to the algorithm is time and this is expressed by a convenient method termed Julian Day. The Julian Day counts whole days since March 1, 4800 B.C, it also aims to simplify and consolidate the time format into one single variable, instead of splitting it into year, months, date, hours, minutes, and seconds. It is obtained by using (1) [26].

$$\begin{aligned} jd = {} & 365.5 \times (y + 4800 + (m - 4)/12) \\ & + (A1 \times (m - 14)^2/12 - (A2y + 3 + 6.25 \times (m - 14)) \\ & + d - A3 - 0.5 + hour/24.0 \end{aligned} \tag{1}$$

where m is the month, y is the year, d is the day of the month and *hour* is the hour of the day in Universal Time in decimal format. The Universal Time or Greenwich Time depends on the earth's rotation and is counted from midnight. The above equation was formulated by Fliegel and Van Flandern but the last two terms were added by Blanco-Muriel *et al*. These terms make it possible to derive decimal form of the Julian day.

The algorithm makes use of ecliptic coordinates to find the position of the sun. The plane of the earth's yearly orbit around the sun is called the ecliptic. The ecliptic coordinates are calculated from the Julian day, by the following set of equations (all angles are in radians) obtained in Blanco-Muriel *et al*.:

$$n = jd - B_1 \tag{2}$$

where n is time measured in days from epoch January 2000, which is Julian date 2451545.0 as seen in Blanco-Muriel *et al*.

$$L\,(meanlongitude) = C_1 + C_2 \times n \tag{3}$$

where the mean longitude is defined as the longitude of a circular and gravitationally free orbiting body with inclination measured as zero as seen in Blanco-Muriel *et al*.

$$g\,(meananomaly) = D_1 + D_2 \times n \tag{4}$$

If the path were circular, it would not be difficult to find the Sun's position. However, since the deviation from the path around the sun is about one degree per day, then the mean anomaly of the Sun is the position of the earth along this path. The true anomaly of the Sun is defined as the position along its real elliptical path is shown in (5).

$$l\,(eclipticlongitude) = L + E_1 \times sin\,(g) + E_2 \times sin(2g) \tag{5}$$

To help visualize the movement of the Sun, astronomers introduced the idea of the celestial sphere. We can imagine the sky as an infinite hollow sphere encompassing the Earth. This imaginary sphere is a very good way to visualize the motion of the sky. Ecliptic longitude is calculated based on the coordinate of the ecliptic system. Here, the ecliptic longitude is denoted as the angular eastward distance measured from the vernal equinox to the intersection of ecliptic. Vernal equinox (March 21 in the northern hemisphere) has a declination of 0 degrees, The vernal equinox marks the first day of spring.

$$\begin{aligned} & ep\,(obliquityoftheecliptic) \\ & \quad = F_1 - F_2 10^{-9} \times n[[space]] + F_3 \times \cos\,(g) \end{aligned} \tag{6}$$

where the *obliquity of the ecliptic* is the angle between the equatorial plane and ecliptic plane. The axial tilt of the earth changes gradually over a thousand of years, but its current value is closely 23degrees 26 mins $23^o16'$.

For the solar tracking system, the equatorial coordinates must be converted into horizontal coordinates to have more meaning and use by the system. This is done by using (7) and (8).

$$ra\,(rightascension) = arctan\left[\frac{cos\,(ep) \times sin\,(l)}{cos\,(l)}\right] \tag{7}$$

$$dec\,(declination) = arcsin[(sin(ep) \times sin(l))] \tag{8}$$

where *ra* denotes the right ascension and *dec* denotes the declination. The unit for right ascension is degrees, but it is commonly measured in time (hours, minutes, and seconds). This means that if the sky rotates 360 degrees in 24 hr, therefore, it turns every hour. For example, 1 hour of right ascension is equivalent to 15 degrees of sky rotation. The celestial equivalent of latitude is called declination and is measured in degrees. North of the celestial equator the declination values are positive and south of the Celestial Equator [26].

$$\begin{aligned} &lmst\ (LocalMeanSiderealTime) \\ &\quad = (gmst \times 15 + longitude) \times (\pi/180) \end{aligned} \tag{9}$$

where *Local Mean Sidereal Time* (LMST) is obtained from the current *Greenwich Mean Sidereal Time* (GMST), with a mean solar day to the mean sidereal day offset in the longitude of 1.00273790935. For the longitude the west of the *Greenwich Meridian* (GM), it is given a negative sign in (9). For the longitude to the east of the GM, the sign of the longitude in (9) is positive. Sidereal time is defined as the hour angle of the vernal equinox. Sidereal time enables measurement of the rotation of the earth with respect to the stars, rather than the Sun. The current GMST should be calculated using the following formula:

$$gmst\ (hours) = G_1 + G_2 \times n + G_3 \times hour \tag{10}$$

where *hour* is the hour of the day in Universal Time in decimal format, for example, 9 h 14 min 55 sec converted to decimals is:

$$\begin{aligned} 9hours14mins55secs &= 9 + \frac{14}{60} + \frac{55}{3600} \\ &= H_1 hours \end{aligned} \tag{11}$$

A conversion from celestial to horizontal coordinates (also known as altitude and azimuth coordinates) is achieved by finding the hour angle. The hour angle is obtained by finding the Local Sidereal Time (LST) as shown in (9), via the Universal Time and longitude of the observer's position, and then subtracting the right ascension from the Local Sidereal Time to obtain the hour angle as shown in (12).

$$wh(hourangle) = lmst - ra \tag{12}$$

Moreover, the following equations in (13) and (14) enable the calculation of Zenith angle θ_Z, and azimuth angle θ_A, of the Sun for an observer at longitude and latitude. where B is the latitude

$$\begin{aligned} \theta_Z\ (zenithangle) &= cos^{-1}[cos(B)cos(wh)cos(dec) \\ &\quad + sin(dec)sin(B)] \end{aligned} \tag{13}$$

$$\begin{aligned} \theta_A\ (azimuthangle) &= tan^{-1}[-sin(wh)/(tan(dec) \times cos(B) \\ &\quad - sin(B) \times cos(wh))] \end{aligned} \tag{14}$$

To deal with parallax by using (15) and (16).

$$Parallax = -4.26 * 10^{-5} \times cos(h) \tag{15}$$

$$\theta_{Z_{new}} = \theta_Z + Parallax \tag{16}$$

When from observing near the horizon, refraction is important, and it is necessary to correct for atmospheric refraction to ensure the highest degree of accuracy is maintained. The Sun approximately 34 minutes below the horizon can still be visible because of refraction. We also need to take the atmospheric pressure and temperature impact on the obtained $\theta_{Z_{new}}$ as follows:

$$\theta_{ref} = \frac{I_1 P}{(273 + T)tan(\theta_{Z_{new}} + I_2/(\theta_{Z_{new}} + I_3))} \tag{17}$$

where P represents the atmosphere pressure in millibars and T represents temperature in Celsius at point of observation. Therefore, the actual zenith angle θ_Z becomes

$$\theta_{Z_{Actual}} = \theta_{ref} \pm \delta \tag{18}$$

where δ represents the measurement impacts caused by the digital compass which has an accuracy of 1-2 degrees and the tilt sensor whose resolution allows for measurements with inclination changes of less than 1 degree. The table 1 shows symbols for the numerical values in the equations. The Table 2 shows a comparison between the original PSA algorithm and the proposed modified PSA algorithm.

C. CALCULATION OF THE ACTUAL MEASURED ZENITH ANGLE OF THE SUN USING SHADOW LENGTH

To be able to calculate the actual Sun angle, first one must measure the height of the pole or stick, and then measure the shadow length of the pole. The Sun's actual measured Zenith angle can be then calculated as follows:

$$\theta_Z = arctan(shadowlength/poleheight) \tag{19}$$

III. EXPERIMENTS AND RESULTS

Figs. 6, 7 and 8 depict the completed mechanical structure of the prototype, the final prototype, and the circuit board, respectively, of our proposed solar-tracking system. The brands and models of motors used in the system are Mabuchi and 550VC respectively. And the brands and models of sensors used in the system are Wit-Motion and SINDT02-485 respectively. When the proposed automatic tracking system is initially put outside, the solar receiving panel rotates — based on the pulse signals from the microcontroller controlling the stepping from the stepper motor — until the perfect position is obtained relative to the Sun. At the end of the day, the control algorithm resets the panel to the previous day initial position.

Experiments were carried out in Tianjin City, daily from 9:00 to 17:00 for a period of one year and the Zenith angle values were measured using right ascension of 0.3529 rads and declination of 0.07016 rads. During this time period, we recorded the actual Zenith angles of the Sun by using the shadow length method discussed with the help of a one-meter measuring rule. After accounting for parallax error, we utilized the trigonometry by using (19) to derive the actual measured Zenith angle, then the obtained readings were

TABLE 1. Symbols for the numerical values in the equations.

A_1=30.5833	A_2=0.0075	A_3=32075
B_1=2451545.0		
C_1=4.8949329	C_2= 0.017202791698	
D_1=6.2400582	D_2=0.0172019699	
E_1=0.33423055	E_2=0.00034906	
F_1=0.4090928	F_2=6.2140	F_3=0.0000396
G_1=6.6208844	G_2=0.0657098283	G_3=1.00273790935
H_1=9.24861111		
I_1=0.084217	I_2=0.0031376	I_3=0.089186

TABLE 2. Comparison of original Blanco-Muriel algorithm versus modified algorithm.

Blanco-Muriel algorithm	Blanco-Muriel modified algorithm
jd=(1461×(y+4800+(m-14)/12+(367×(m-2-12×((m-14)/12)))/12-3×((y+4900+(m-14)/12)/100))/4+d-32075-0.5+hour/24.0)	jd=365.5×(y+4800+(m-4)/12) +(A_1×(m-14)^2/12 − (A_2 y + 3 + 6.25 × (m − 14)) + d − A_3 − 0.5 + hour/24.0
$n = jd - 2451545.0$	$n = jd - B_1$
$L(mean\ longitude) = 4.8950630 + 0.017202791698 \times n$	$L(mean\ longitude) = C_1 + C_2 \times n$
$g(mean\ anomaly) = 6.2400600 + 0.0172019699 \times n$	$g(mean\ anomaly) = D_1 + D_2 \times n$
$l(ecliptic\ longitude) = L + 0.03341607 \times sin(g) + 0.00034894 \times sin(2g) - 0.0001134 - 0.0000203 \times sin(g)$	$l(ecliptic\ longitude) = L + E_1 \times sin(g) + E_2 \times sin(2g)$
$ep(obliquity\ of\ the\ ecliptic) = 0.4090928 - 6.2140 * 10^{-9} \times n + 0.0000396 \times cos(g)$	$ep(obliquity\ of\ the\ ecliptic) = F_1 - F_2 * 10^{-9} \times n + F_3 \times cos(g)$
$gmst(Greenwich\ Mean\ Sidereal\ Time) = 6.6974243242 + 0.0657098283 \times n + hour$	$gmst(hours) = G_1 + G_2 \times n + G_3 \times hour$
$lmst(Local\ Mean\ Sidereal\ Time) = (gmst \times 15 + longitude) \times (\pi/180)$	$lmst(Local\ Mean\ Sidereal\ Time) = (gmst \times 15 + longitude) \times (\pi/180)$
$wh(hour\ angle) = lmst - ra$	$wh(hour\ angle) = lmst - ra$
$\theta_Z(zenith\ angle) = arccos[cos(latitude) \times cos(wh) \times cos(dec) + sin(dec) \times sin(latitude)]$	$\theta_Z(zenith\ angle) = cos^{-1}[cos(B)\,cos(wh)\,cos(dec)) + sin(dec)sin(B)]$
Parallax=[EarthMeanRadius×sin(θ_Z)]/$AstronomicalUnit$	Parallax=-4.26*$10^{-5} \times cos(h)$
Not considered	$\theta_{Z_{new}} = \theta_Z + Parallax$
Not considered	$= \frac{\theta_{ref}\ I_1 P}{(273+T)tan(\theta_{Z_{new}} + I_2/(\theta_{Z_{new}} + I_3))}$

recorded and plotted in Fig. 10. Fig. 10 shows a comparison between the PSA modified algorithm and the original algorithm in Zenith angle at different moments of the same day. Fig. 9 shows a comparison between the PSA modified

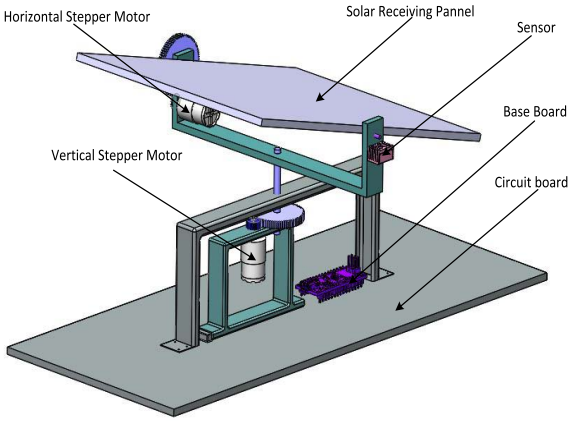

FIGURE 6. Mechanical structure of solar auto-tracking system.

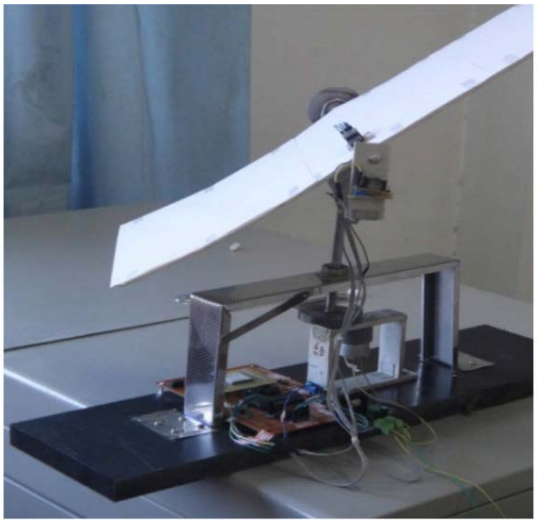

FIGURE 7. Final solar tracking prototype.

algorithm and the original algorithm in Zenith angle at different moments of the same day. The red line represents the value of the curve calculated by PSA modified algorithm and the blue line represents the value of the curve calculated by PSA original algorithm in Fig. 9. The red line represents the actual valueof the Zenith angle by the automatic solar tracking system and the blue line in represents the value of the curve calculated by PSA modified algorithm in Fig. 10. For better comparison, the results of the actual Zenith angle values and the PSA modified algorithm calculations are plotted against each other by simulation in MATLAB, as shown in Fig. 10.

We can see from Fig. 9 that the Blanco-Muriel modified algorithm achieves better accuracy than its original algorithm and the original algorithm has a different shape to the modified one, this is due to the original algorithm being valid between the periods of 1999-2015, after 2015, the original algorithm becomes inaccurate as can be seen in Fig. 10. Our result confirms the findings in Blanco *et al.*, 2020. Here, we observe that the minimum Zenith angle occurs two and a half hours after local noon. Therefore, it is essential to develop a new algorithm with better accuracy response.

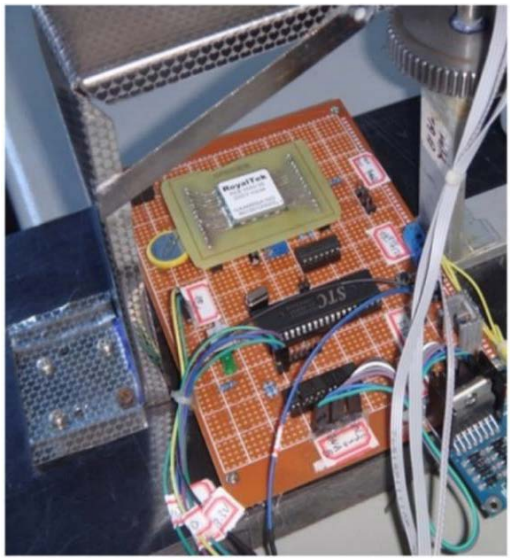

FIGURE 8. Circuit board of solar tracking system.

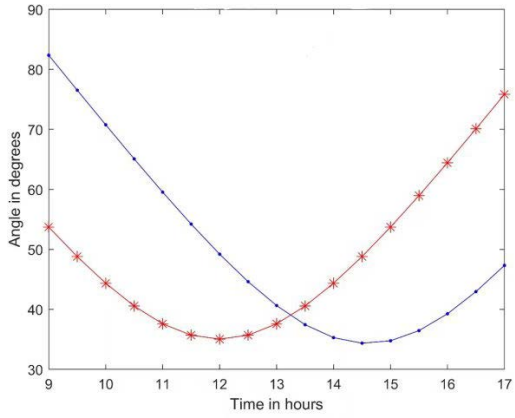

FIGURE 9. PSA modified algorithm compared against the original one in Zenith angle.

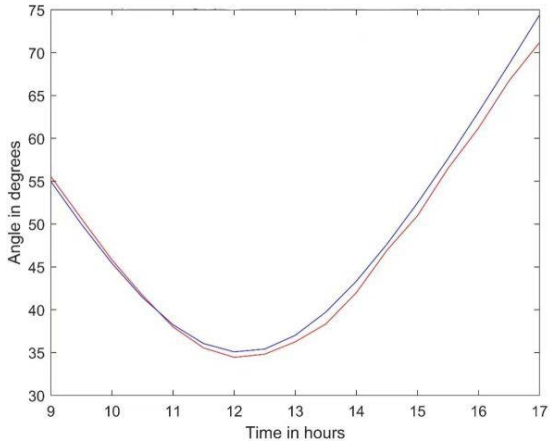

FIGURE 10. Actual measurement and calculating measurement of Zenith angle.

Furthermore, in Fig. 10, the actual value of the Zenith angle is so close to the calculated value which proves the automatic solar tracking system is successful and works well.

IV. CONCLUSION

In this paper, a new automatic tracking system with two-axis based on the PSA modified algorithm is designed and based on which lots of experiments are carried out in Tianjin City, China. Then Zenith, angle values are recorded and relative results are analyzed. The research about solar energy and methods of solar tracking system design in domestic and foreign regions is introduced and compared. From the obtained results, we observed that the modified PSA algorithm is more accurate in calculating the Sun's position than the original algorithm. In this article, we present the flowchart of the automatic tracking system and its working principle among these modules is explained in brief. Then, the biaxial tracking is designed and utilized and the control system is placed on the board at the bottom of the whole mechanical structure. The circuit system consists of a tilt sensor, microcontroller, digital compass, GPS module and other key components. At last, the system is designed successfully and experiments are carried out in Tianjin City. Then a comparison plot containing Zenith angle values shows that the automatic solar tracking system achieves good performance and the PSA modified algorithm is suitable to replace the original algorithm.

The modified PSA algorithm is based on universal Earth-Sun geometry and atmospheric concepts that are applicable in both hemispheres, and the system can be deployed in any country and still achieve good tracking performance as well as being useful to the academic and industrial community in developing countries looking for low-cost innovative tracking solutions. Even though, in recent years, sun-tracking PV panels are rarely seen in practice as the cost of PV panels has dramatically decreased in the past five years. However, accurate sun-tracking is still important for high solar concentrating systems and our proposed algorithm can provide potential benefit for such systems due to the improvement in sun-tracking provided by our solution.

REFERENCES

[1] J.-C. Wu, H.-L. Jou, W.-C. Wu, and C.-H. Chang, "Solar power generation system with power smoothing function," *IEEE Access*, vol. 10, pp. 29982–29991, 2022.

[2] A. Z. Hafez, A. M. Yousef, and N. M. Harag, "Solar tracking systems: Technologies and trackers drive types—A review," *Renew. Sustain. Energy Rev.*, vol. 91, pp. 754–782, Aug. 2018.

[3] P. Sharma and N. Malhotra, "Solar tracking system using microcontroller," in *Proc. 1st Int. Conf. Non Conventional Energy (ICONCE)*, Coimbatore, India, Jan. 2014, pp. 1094–1098.

[4] F. I. Mustafa, A. S. Al-Ammri, and F. F. Ahmad, "Direct and indirect sensing two-axis solar tracking system," in *Proc. 8th Int. Renew. Energy Congr. (IREC)*, Amman, Jordan, Mar. 2017, pp. 1–4.

[5] W. Nsengiyumva, S. G. Chen, L. Hu, and X. Chen, "Recent advancements and challenges in solar tracking systems (STS): A review," *Renew. Sustain. Energy Rev.*, vol. 81, pp. 250–279, Jan. 2018.

[6] S. Racharla and K. Rajan, "Solar tracking system—A review," *Int. J. Sustain. Eng.*, vol. 10, no. 2, pp. 72–81, 2016.

[7] P. Sahu, N. S. Maurya, and S. Sahu, "Automatic sun tracking for the enhancement of efficiency of solar energy system," in *Proc. Int. Conf. Utility Exhib. Green Energy Sustain. Develop. (ICUE)*, Phuket, Thailand, Oct. 2018, pp. 1–4.

[8] R. K. Dhar, A. Merabet, A. Al-Durra, and A. M. Y. M. Ghias, "Power balance modes and dynamic grid power flow in solar PV and battery storage experimental DC-link microgrid," *IEEE Access*, vol. 8, pp. 219847–219858, 2020.

[9] G. Perveen, P. Anand, and A. Kumar, "Performance evaluation of solar tracking system," in *Proc. Int. Conf. Smart Technol. Comput., Electr. Electron. (ICSTCEE)*, Bengaluru, India, Oct. 2020, pp. 163–168.

[10] J. Sanjaya, M. A. Dhaneswara, D. V. Hauten, and H. Santoso, "Implementation of solar tracking system to maximize energy absorption in wireless sensor network," in *Proc. 10th Int. Conf. Inf. Technol. Electr. Eng. (ICITEE)*, Bali, Indonesia, Jul. 2018, pp. 577–580.

[11] A. H. Mohaimin, M. R. Uddin, and F. K. Law, "Design and fabrication of single-axis and dual-axis solar tracking systems," in *Proc. IEEE Student Conf. Res. Develop. (SCOReD)*, Selangor, Malaysia, Nov. 2018, pp. 1–4.

[12] F. I. Mustafa, S. Shakir, F. F. Mustafa, and A. T. Naiyf, "Simple design and implementation of solar tracking system two axis with four sensors for baghdad city," in *Proc. 9th Int. Renew. Energy Congr. (IREC)*, Hammamet, Tunisia, Mar. 2018, pp. 1–5.

[13] H. A. E.-M. Salama and A. T. Mohamed Taha, "Practical implementation of dual axis solar power tracking system," in *Proc. 20th Int. Middle East Power Syst. Conf. (MEPCON)*, Cairo, Egypt, Dec. 2018, pp. 446–451.

[14] D. A. Flores-Hernández, S. I. Palomino-Resendiz, A. Luviano-Juárez, N. Lozada-Castillo, and O. Gutiérrez-Frías, "A heuristic approach for tracking error and energy consumption minimization in solar tracking systems," *IEEE Access*, vol. 7, pp. 52755–52768, 2019.

[15] C.-Y. Lee, P.-C. Chou, C.-M. Chiang, and C.-F. Lin, "Sun tracking systems: A review," *Sensors*, vol. 9, no. 5, pp. 3875–3890, 2009.

[16] C. Alexandru, "Optimizing the control system of a single-axis sun tracking mechanism," in *Proc. MATEC Web Conf.*, vol. 184, 2018, pp. 1–4.

[17] A. A. Elsayed, E. E. Khalil, M. A. Kassem, and O. A. Huzzayin, "A novel mechanical solar tracking mechanism with single axis of tracking for developing countries," *Renew. Energy*, vol. 170, pp. 1129–1142, Jun. 2021.

[18] S. A. Pelaez, C. Deline, P. Greenberg, J. S. Stein, and R. K. Kostuk, "Model and validation of single-axis tracking with bifacial PV," *IEEE J. Photovolt.*, vol. 9, no. 3, pp. 715–721, May 2019.

[19] A. Sharma, V. Vaidya, and K. Jamuna, "Design of an automatic solar tracking controller: Solar tracking controller," in *Proc. Int. Conf. Power Embedded Drive Control (ICPEDC)*, Chennai, India, Mar. 2017, pp. 505–510.

[20] C. Hua and J. Lin, "A modified tracking algorithm for maximum power tracking of solar array," *Energy Convers. Manage.*, vol. 45, no. 6, pp. 911–925, Apr. 2004.

[21] Z. Er and S. Marangozoglu, "New design for solar panel tracking system based on solar calculations," in *Proc. IEEE 61st Int. Midwest Symp. Circuits Syst. (MWSCAS)*, Aug. 2018, pp. 1042–1045.

[22] M. E. H. Chowdhury, A. Khandakar, B. Hossain, and R. Abouhasera, "A low-cost closed-loop solar tracking system based on the sun position algorithm," *J. Sensors*, vol. 2019, no. 8, pp. 1–11, Feb. 2019.

[23] A. Ruelas, N. Velázquez, C. Villa-Angulo, A. Acuña, P. Rosales, and J. Suastegui, "A solar position sensor based on image vision," *Sensors*, vol. 17, no. 8, p. 1742, Jul. 2017.

[24] J. A. Carballo, J. Bonilla, M. Berenguel, J. Fernández-Reche, and G. García, "New approach for solar tracking systems based on computer vision, low cost hardware and deep learning," *Renew. energy.*, vol. 133, pp. 1158–1166, 2019.

[25] D. Hoadley, "Efficient calculation of solar position using rectangular coordinates," *Sol. Energy*, vol. 220, pp. 80–87, May 2021.

[26] M. Blanco-Muriel, D. C. Alarcón-Padilla, T. López-Moratalla, and M. Lara-Coira, "Computing the solar vector," *Sol. Energy*, vol. 70, no. 5, pp. 431–441, 2001.

[27] M. J. Blanco, K. Milidonis, and A. M. Bonanos, "Updating the PSA sun position algorithm," *Sol. Energy*, vol. 212, pp. 339–341, Dec. 2020.

[28] R. Grena, "Five new algorithms for the computation of sun position from 2010 to 2110," *Sol. Energy*, vol. 86, no. 5, pp. 1323–1337, May 2012.

[29] R. Ibrahim and A. Afshin, "Solar position algorithm for solar radiation applications," *Sol. Energy Phoenix Arizona Then New York*, vol. 76, no. 5, pp. 577–589, 2004.

[30] V. Poulek, "Testing the new solar tracker with shape memory alloy actors," in *Proc. IEEE 1st World Conf. Photovoltaic Energy Convers.-WCPEC (A Joint Conf. PVSC, PVSEC PSEC)*, Dec. 1994, pp. 1131–1133.
[31] M. J. Clifford and D. Eastwood, "Design of a novel passive solar tracker," *Sol. Energy*, vol. 77, no. 3, pp. 269–280, Sep. 2004.

XIAO LI is currently pursuing the master's degree with the School of Electronic Engineering, Tianjin University of Technology and Education. Her research interests include development of intelligent instruments, mechatronic systems, and robotic systems.

LIQIANG WANG currently works with the School of Electronic Engineering, Tianjin University of Technology and Education, as the Executive Deputy Director of the Tianjin Fieldbus Control Technology Engineering Center. He is an Associate Professor. His research interests include development of intelligent instruments, robotics, intelligent manufacturing, and new technologies of the Internet of Things.

MUNYARADZI MUNOCHIVEYI was born in Harare, Zimbabwe. He received the B.S. degree in electrical engineering from the University of Cape Town, in 2007, the M.S. degree in electronic engineering from the Tianjin University of Technology and Education, Tianjin, China, in 2012, and the D.Eng. degree in communication and information systems from Jilin University, Changchun, China, in 2017. He is currently a Senior Lecturer with the University of Zimbabwe and a Research Assistant with the WICOM Laboratory led by Dr. Thuan. His research interests include wireless communications, machine learning, and robotics.